

RESEARCH

Open Access



The histone deacetylase *Cfhos2* is a key epigenetic factor regulating appressorium development and pathogenesis in apple *Glomerella* leaf spot fungus *Colletotrichum fructicola*

Mengyu Cao, Zhaohui Zhang, Huanhuan Tian, Wei Yu, Xuemei Zhao, Wenrui Yang, Rong Zhang, Guangyu Sun and Xiaofei Liang* 

Abstract

Glomerella leaf spot (GLS) is a devastating fungal disease that damages the leaves and fruits and reduces tree vigor of apple (*Malus domestica*). The pathogen infection mechanism, however, remains elusive. Histone-modifying enzymes, which regulate eukaryotic chromatin conformation and gene expression, are key epigenetic factors controlling fungal development, virulence, and secondary metabolism. To dissect the epigenetic regulation of GLS pathogenesis, we characterized a histone deacetylase gene *Cfhos2* in *Colletotrichum fructicola*, the causing agent of GLS. *Cfhos2* deletion mutants were mildly reduced in vegetative growth rate, but almost lost pathogenicity on apple leaves. *Cfhos2* deletion mutants induced strong plant defense responses manifested by epidermal cell browning, granulation, and distortion of pathogen invasive hyphae. The mutants also showed defect in appressorial development on cellophane, but not on parafilm or on apple leaf surface, suggesting that the defect in appressorial development is surface-dependent. RNA-seq based transcriptome analysis highlighted that *Cfhos2* regulates secondary metabolism-related virulence genes during infection. Moreover, the expression of an apple defense-related F-box protein was strongly induced by infection with *Cfhos2* deletion mutants. Taken together, we demonstrate that *Cfhos2* is a key epigenetic factor regulating appressorium development, virulence gene expression, and GLS pathogenesis in *C. fructicola*. The results provide important information for understanding the virulence mechanisms of *C. fructicola*.

Keywords: Histone deacetylase, *Colletotrichum fructicola*, Virulence

Background

Fungal pathogenesis is a sophisticated process including infectious development of the pathogen and fungus–host interactions, which requires a fine-tuned regulation of gene expression dynamics. Histones are

conserved eukaryotic proteins that pack DNA into a compact structure called chromatin. Covalent histone N-terminal modifications, such as acetylation, phosphorylation, methylation, and ubiquitination, alter chromatin architectures and impact various cellular aspects encompassing gene transcription, genome replication, DNA damage repair, and cell cycle (Tessarz and Kouzarides 2014; Dubey and Jeon 2017; Lai et al. 2022). Among all types of histone modifications, the reversible N-terminal lysine acetylation, regulated by histone acetyltransferase

*Correspondence: xiaofeilang@nwsuaf.edu.cn

State Key Laboratory of Crop Stress Biology in Arid Areas, College of Plant Protection, Northwest A&F University, Yangling 712100, China



© The Author(s) 2022. **Open Access** This article is licensed under a Creative Commons Attribution 4.0 International License, which permits use, sharing, adaptation, distribution and reproduction in any medium or format, as long as you give appropriate credit to the original author(s) and the source, provide a link to the Creative Commons licence, and indicate if changes were made. The images or other third party material in this article are included in the article's Creative Commons licence, unless indicated otherwise in a credit line to the material. If material is not included in the article's Creative Commons licence and your intended use is not permitted by statutory regulation or exceeds the permitted use, you will need to obtain permission directly from the copyright holder. To view a copy of this licence, visit <http://creativecommons.org/licenses/by/4.0/>.

(HAT) and histone deacetylase (HDAC), is one of the best-characterized machineries (Kurdistani and Grunstein 2003). HDACs function by removing acetyl residues from the ϵ -amino group of lysine residues in the histone N-terminal tail, which restores the positive charge on the histone (Lai et al. 2022). Such positive charge generally facilitates histone-DNA binding, thereby favors chromatin condensation and transcriptional repression (Bannister and Kouzarides 2011), but in rare case leads to transcription activation as well (Wang et al. 2002). Fungal HDACs can be classified into two main groups based on their coactivator dependency: (i) Zn(II)-dependent, or 'classical' HDACs, including Hda1, Hos1, Hos2, Hos3, and Rpd3 in *Saccharomyces cerevisiae*; (ii) NAD⁺-dependent, or Sir2 (silent information regulator 2) family, with Sir2 in *S. cerevisiae* as the founding member (Jeon et al. 2014). Different HDACs interact with different sets of proteins and form distinct HDAC protein complexes, which function differently in terms of the histone and lysine sites being modified, the targeted genomic regions, and the associated biological effects (Jeon et al. 2014).

Set3C represents one of the most conserved and best characterized HDAC complexes in fungi. The core components of Set3C in *Saccharomyces cerevisiae* include Hos2, Set3, Snt1, and YIL112w (Pijnappel et al. 2001), which are also conserved in *Schizosaccharomyces pombe* (Wirén et al. 2005), *Magnaporthe oryzae* (Ding et al. 2010), *Fusarium graminearum* (Li et al. 2011), and *Candida albicans* (Hnisz et al. 2012). Functionally, Set3C/Hos2 is a key virulence regulator, and deletion of *hos2* or other Set3C component affects the virulence of *M. oryzae* (Ding et al. 2010), *Cochliobolus carbonum* (Baidyaroy et al. 2001), *F. graminearum* (Li et al. 2011), *Beauveria bassiana* (Cai et al. 2018), *Ustilago maydis* (Elías-Villalobos et al. 2015), and *C. albicans* (Hnisz et al. 2010). In *Aspergillus* spp. and *Fusarium fujikuro*, Set3C/Hos2 also regulates the biosynthesis of secondary metabolites including aflatoxin, orsellinic acid, and gibberellin (Studt et al. 2013; Pidroni et al. 2018; Lan et al. 2019). Hos2-mediated HDAC activity causes deacetylation of H4-K16 and H3-K18 (Jeon et al. 2014; Lai et al. 2022), with the binding and modifications mainly locating within the gene-coding regions, and correlating with changes in expression or induction kinetics of target genes (Wang et al. 2002; Wirén et al. 2005; Hnisz et al. 2012).

Glomerella leaf spot (GLS) of apple is a destructive fungal disease that severely damages apple (*Malus domestica*) production (Taylor 1971; Velho et al. 2019). The disease was first reported in the United States in 1970s (Taylor 1971) and subsequently in Brazil, Uruguay, and China (Wang et al. 2012; Rockenbach et al. 2016). Under favorable weather conditions (high temperature and

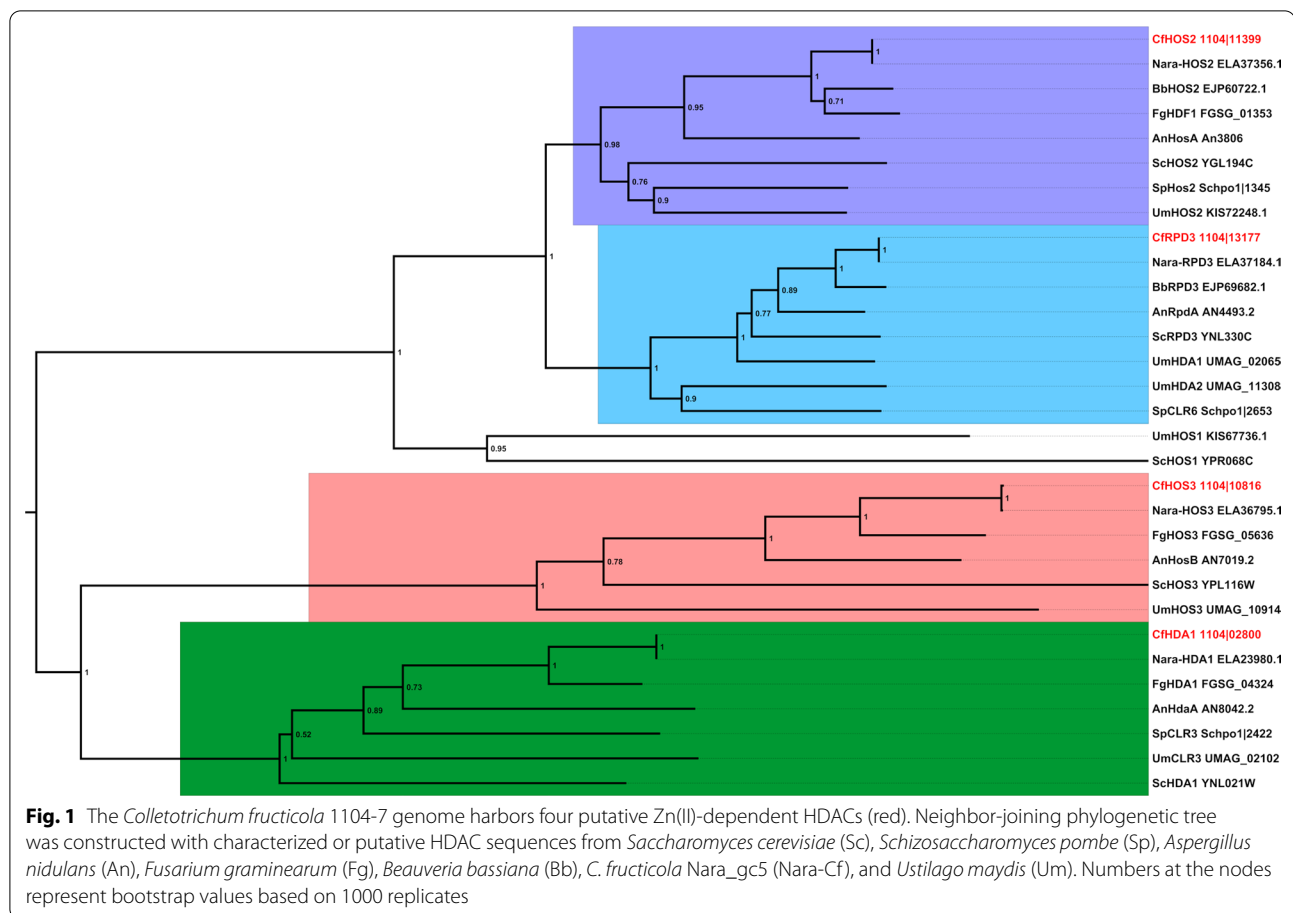
humidity), GLS leads to rapid and massive leaf necrosis and defoliation (Hamada et al. 2019). GLS also causes small sunken lesions (1–3 mm) on apple fruit, which considerably lowers fruit quality and commodity value. Massive GLS defoliation weakens tree vigor and reduces fruit setting in the following year. In China, GLS was first reported in 2010, but due to its rapid spread, the disease has now become an important threat to commercial apple production in the whole country (Wang et al. 2012). GLS disease is caused by *Colletotrichum* species, with *C. fructicola* being the dominant species in multiple regions (Weir et al. 2012; Velho et al. 2019).

Currently, limited knowledge is known regarding the fungal pathogenicity mechanisms in causing GLS. Histological and ultrastructural studies on GLS have revealed a hemibiotrophic infection mode of *C. fructicola* involving the development of various infection structures and the dynamic expression of virulence genes (Liang et al. 2018a; Shang et al. 2020), which implies the involvement of delicate gene expression control. Previously, we have shown that a putative class I HDAC (*Cfhos2*) is important for sexual reproduction in *C. fructicola* (Liang et al. 2021). However, the importance of this gene in fungal virulence has not been determined. Moreover, the *C. fructicola* genome contains three additional class I HDACs that have not been characterized. In this study, we determined the virulence functions of all these four HDACs in *C. fructicola* by gene deletion analysis and identified *Cfhos2* as a key regulator of appressorium development and plant infection, we also dissected the virulence functions of *Cfhos2* with a combination of histological and transcriptomic methods. Our study results highlight the involvement of epigenetic factors in regulating the pathogenesis of *C. fructicola*, and perhaps other *Colletotrichum* pathogens as well.

Results

The *C. fructicola* genome encodes four putative histone deacetylases belonging to the Rpd3/Hda1 family

To identify the putative HDACs in *C. fructicola*, we performed a local BLASTp search against the published *C. fructicola* genome (Liang et al. 2018b) with the AnHosA protein from *Aspergillus nidulans* (Pidroni et al. 2018) as a query. Four homologous proteins, 1104|11399, 1104|13177, 1104|10816, and 1104|02800, were identified, which showed 63.4%, 48.1%, 36.5%, and 31.1% amino acid identity, respectively, with AnHosA. All these four proteins contain an HDAC domain (PF00850). Phylogenetic analysis of the selected fungal HDACs identified four major clades, each containing one of the four *C. fructicola* proteins (Fig. 1). Based on the phylogenetic pattern, the four *C. fructicola* proteins were named CfhOS2 (1104|11399), CfrPD3 (1104|13177), CfhOS3



(1104|10816), and CfHDA1 (1104|02800), showing 48.5%, 73.1%, 41.6%, and 38.4% amino acid identity with the corresponding *S. cerevisiae* orthologues, respectively.

Deletion of *Cfhos2* in *C. fructicola* affects stress tolerance, appressorium development, and appressorium-mediated penetration

We performed gene deletion analysis to dissect the biological functions of the four identified class I HDACs in *C. fructicola*. *Cfhos2* deletion mutants were generated previously (Liang et al. 2021), and here the targeted gene deletion events were further confirmed by Southern blot (Additional file 1: Figure S1). Our attempt to generate *Cfryp3* deletion mutant failed whereas *Cfhos3* deletion mutants and *Cfhda1* deletion mutants were successfully obtained. Compared with the wild-type *C. fructicola* strain (WT), no obvious phenotypic change was observed for *Cfhos3* or *Cfhda1* deletion mutants in terms of vegetative growth rate, sensitivity to trichostatin A (TSA, a HDAC inhibitor), and pathogenicity against apple plants (Additional file 1: Figure S2). Moreover, deletion of *Cfhos3* or *Cfhda1* did not affect conidial germination, in vitro infection structure development (appressorium,

infectious hyphae), and fungal tolerance toward osmotic, membrane, cell wall, and oxidative stresses (Additional file 1: Figure S3). Differing from *Cfhos3* and *Cfhda1*, *Cfhos2* deletion mutants showed TSA hypersensitivity and severely reduced virulence (detailed below).

On potato dextrose agar (PDA) medium, the two *Cfhos2* deletion mutants, Δ *hos2-4* and Δ *hos2-5*, were defective in vegetative growth (Fig. 2a), with a growth rate of approximately 80% of that of WT (1104-6), and the mutant colonies were melanized to a reduced degree. These defects, however, were fully complemented in the complementation strain, *hos2-4-3*. In *U. maydis* and *S. pombe*, deletion of HDACs led to hypersensitivity of the mutants toward the HDAC inhibitor TSA (Olsson et al. 1998; Elías-Villalobos et al. 2015). Similarly, *Cfhos2* deletion mutants (Δ *hos2-4* and Δ *hos2-5*) were approximately 1.7- and 2.5-fold more sensitive to TSA relative to WT and the complementation strain (*hos2-4-3*), respectively (Fig. 2a, b). Compared with the WT and complementation strains, Δ *hos2-4* and Δ *hos2-5* were hypersensitive to the cell wall stress agent Congo red (CR) and alkaline stress (pH 8.0) (Fig. 3), whereas behaved similarly under osmotic stresses (NaCl, KCl, sorbitol), oxidative

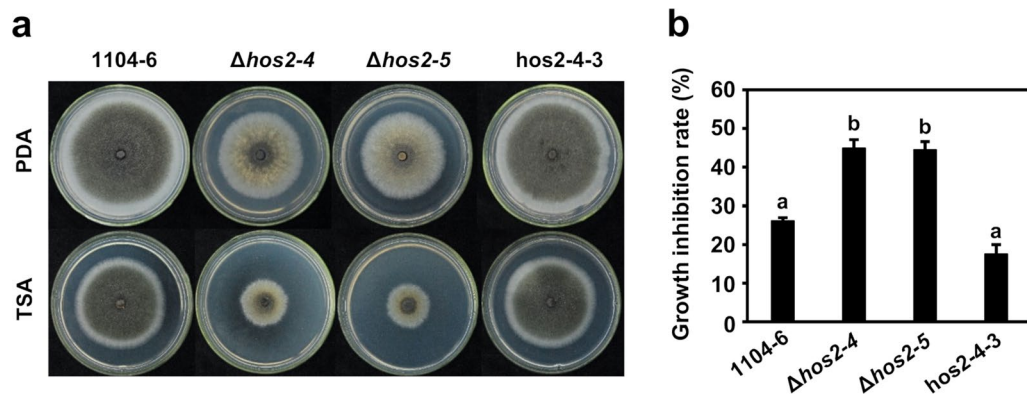


Fig. 2 *Cfhos2* regulates colony morphology and trichostatin A (TSA) sensitivity. **a** Colony morphologies of WT (1104-6), *Cfhos2* deletion mutants (Δ hos2-4, Δ hos2-5), and the complementation strain (hos2-4-3) grown on PDA or on PDA supplemented with the HDAC inhibitor TSA (1 μ g/mL) at 25 °C for 6 days. **b** Relative growth inhibition of different strains by TSA on PDA as calculated from colony diameters grown for 5 days. Means + standard deviations ($n = 3$) were plotted, and different letters indicate groups with significant statistical difference (adjusted $P < 0.05$) based on Tukey's multiple comparison test following one-way ANOVA

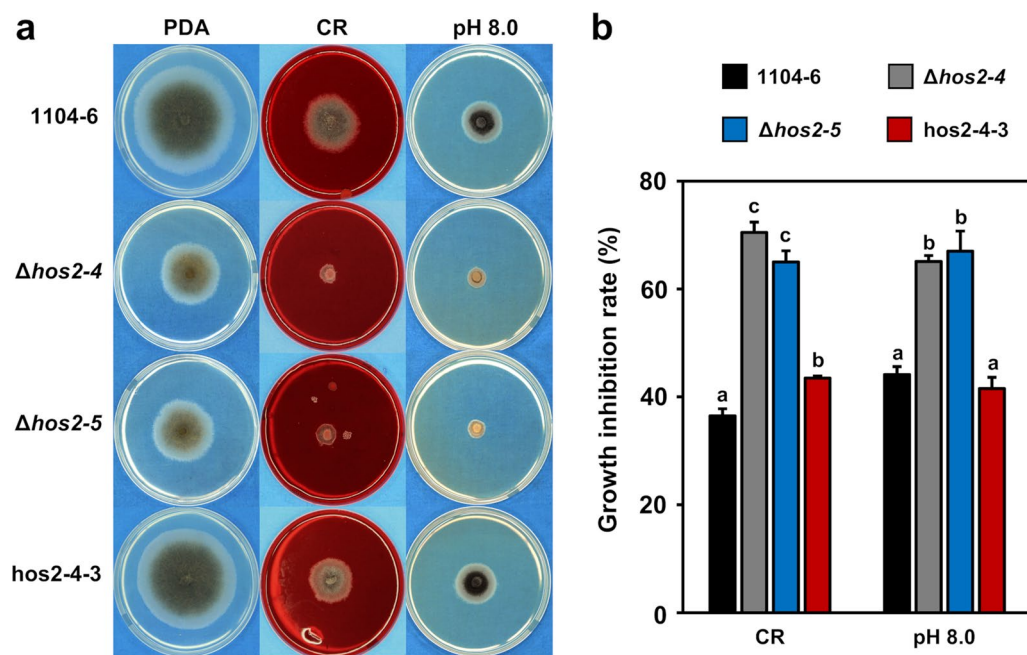


Fig. 3 *Cfhos2* deletion mutants are hypersensitive to Congo red (CR) and alkaline stress (pH=8.0). **a** Colony morphologies of selected strains on PDA, PDA amended with 1000 μ g/mL CR, or PDA buffered at pH 8.0 for 4 days. **b** Barplot showing variation in growth inhibition of different strains to the indicated stresses. Means + standard deviations ($n = 3$) were plotted, and different letters indicate groups with significant statistical difference (adjusted $P < 0.05$) based on Tukey's multiple comparison test following one-way ANOVA

stress (H_2O_2), cell membrane damage stress (0.2% SDS), and acidic stress (pH 3.0) (Additional file 2: Table S1). When cultured on medium with carboxymethyl cellulose (CMC) as the sole carbon source, *Cfhos2* deletion mutants showed more severe growth inhibition (Additional file 2: Table S1), but no obvious growth inhibition

was observed on minimum (nutrient poor) medium (MM) or medium supplemented with pectin as the sole carbon source (Additional file 2: Table S1), compared with WT and complementation strains.

Deletion of *Cfhos2* did not affect conidial yield of *C. fructicola*. On cellophane overlaid agar medium (2%

agar), conidial germination rates of $\Delta hos2-4$ and $\Delta hos2-5$ strains were $68 \pm 10\%$ and $69 \pm 2\%$ after incubation for 12 h, respectively, which were lower but not significantly different from those of 1104-6 ($79 \pm 3\%$) and *hos2-4-3* ($79 \pm 3\%$) strains. On the contrary, appressorium development and cellophane penetration rates of $\Delta hos2-4$ and $\Delta hos2-5$ were drastically reduced compared with those of WT and complementation strains (Fig. 4a, b). At 18 h after incubation, appressorium formation rates of $\Delta hos2-4$ and $\Delta hos2-5$ were $6 \pm 1\%$ and $5 \pm 2\%$, respectively, whereas those of 1104-6 and *hos2-4-3* were $89 \pm 9\%$ and $97 \pm 1\%$, respectively; similarly, the penetration rates of $\Delta hos2-4$ and $\Delta hos2-5$ at this time point were $17 \pm 6\%$ and $18 \pm 2\%$, respectively, much lower than those of 1104-6 ($93 \pm 3\%$) and *hos2-4-3* ($98 \pm 1\%$) (Fig. 4a, b). In sum, *Cfhos2* deletion did not affect conidial production and germination, but dramatically reduced appressorium differentiation and appressorium-mediated penetration on cellophane membrane.

To our surprise, $\Delta hos2-4$ and $\Delta hos2-5$ had similar efficiency in appressorium differentiation as that of WT on parafilm or on apple leaf surface (Fig. 4b), indicating that *Cfhos2* regulates appressorium differentiation in a surface-dependent manner. In *Colletotrichum* fungi, the formation of conidial anastomosis tubes (CATs) has been reported in several species including *C. fructicola* (Gonçalves et al. 2016; Mehta and Baghela 2021). The formation of CATs, however, was not obviously observed in either WT or the $\Delta Cfhos2$ mutants regardless of whether they were incubated on cellophane membrane or on apple leaf surface (Fig. 4b). In a previous study, CATs formation was observed in fruit-derived but not leaf-derived isolates of *C. fructicola* (Gonçalves et al. 2016), indicating intraspecific variability of *C. fructicola* in the capacity to form CATs.

Cfhos2 encodes a key pathogenic factor in *C. fructicola* with post-invasive functions

In leaf infection assays, apple leaves spray-inoculated with conidial suspension (1×10^7 conidia/mL) of $\Delta hos2-4$ or $\Delta hos2-5$ showed almost no symptom except for tiny, pinhole-sized lesions (Fig. 5a), whereas 1104-6 and *hos2-4-3* caused necrotic lesions, which rapidly expanded and merged, resulting in withering of the whole leaves. Similar symptom differences were also observed when apple leaves were drop-inoculated with conidial suspensions (Fig. 5b), or when apple fruits were spray-inoculated with conidial suspensions (Fig. 5c). Importantly, wounding treatment prior to inoculation did not restore the pathogenicity defect of $\Delta hos2-4$ and $\Delta hos2-5$ (Fig. 5d), supporting that *Cfhos2* is a critical pathogenic factor with post-invasion functions. $\Delta hos2-4$ and $\Delta hos2-5$ also showed virulence defect toward wounded pear fruit

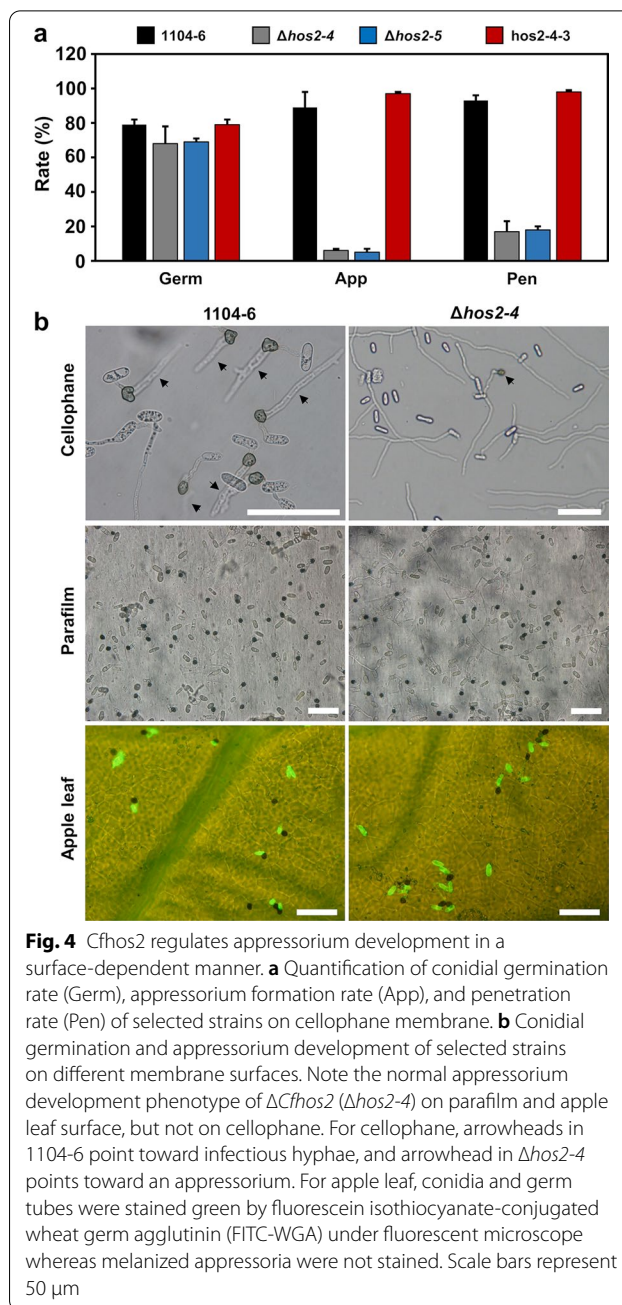


(Fig. 5e), and lesion diameters incurred by the mutants were around 60% of that of WT (Fig. 5f).

Cfhos2 deletion leads to enhanced plant defense responses

To further dissect the pathogenic functions of *Cfhos2*, we compared the histological changes in apple leaf tissues at 2 and 4 days post-inoculation (dpi) with 1104-6 or $\Delta hos2-4$. The infectious hyphae were visualized with the aid of fluorescein isothiocyanate-conjugated wheat germ agglutinin (FITC-WGA) fluorescence staining (Fig. 6). At the

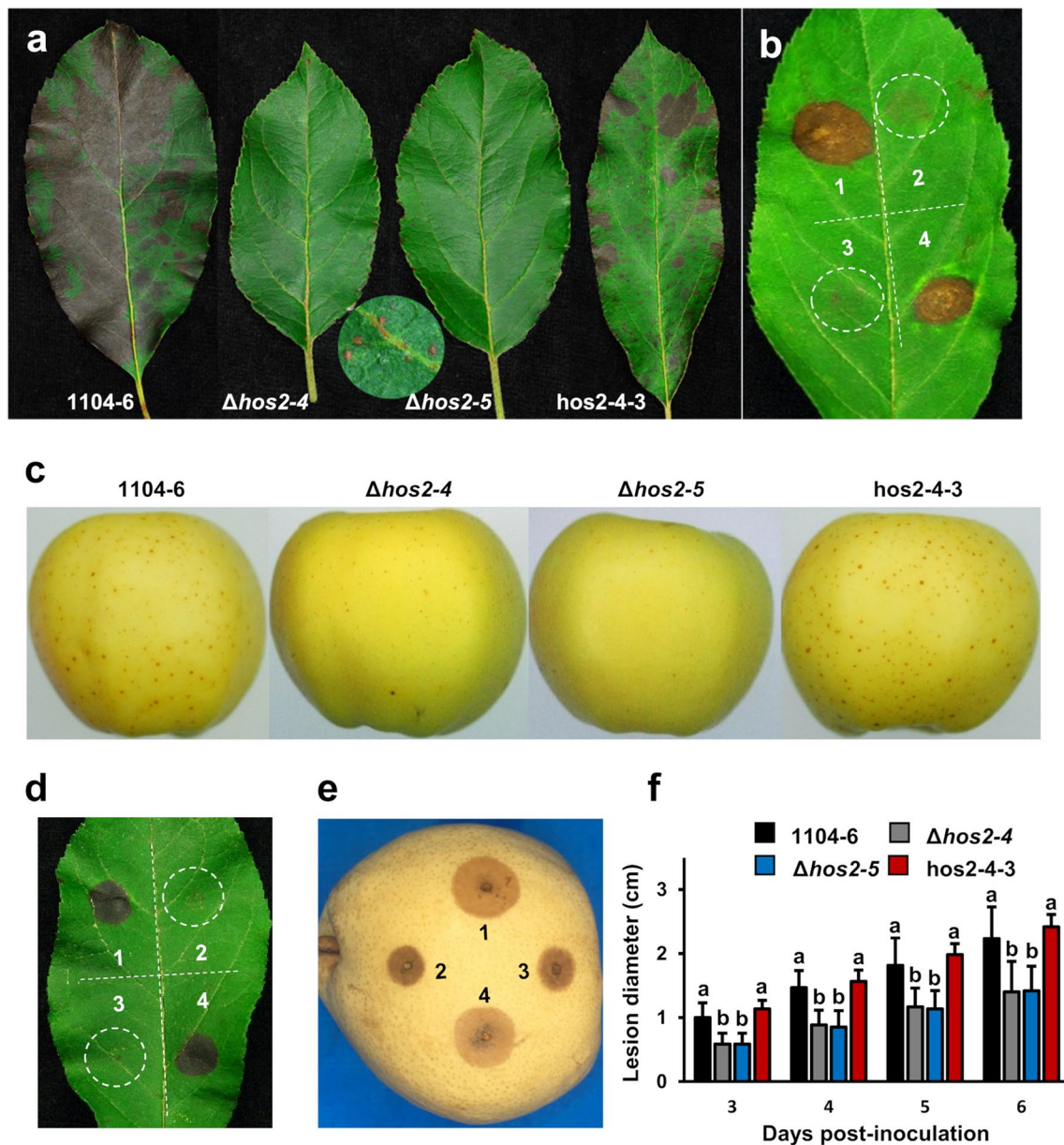


Fig. 5 *Cfhos2* is a key virulence factor. **a** Apple leaves spray-inoculated with conidial suspensions (1×10^7 conidia/mL) at 5 days post-inoculation (dpi). **b** An apple leaf drop-inoculated with conidial suspensions at 5 dpi. 1 to 4 represent WT (1104-6), $\Delta Cfhos2$ ($\Delta hos2-4$, $\Delta hos2-5$), and the complementation strain (*hos2-4-3*), respectively. **c** Apple fruits spray-inoculated with conidial suspensions at 6 dpi. **d** A leaf wound-inoculated with mycelial plugs at 5 dpi, with the same inoculation order as in **b**. **e** A pear fruit wound-inoculated with mycelial plugs at 6 dpi, with the same inoculation order as in **b**. **f** Quantification of lesion size on wound-inoculated pear fruit at different time points. Multiple comparison following ANOVA analysis was performed, error bar indicates standard deviation ($n = 3$), and different letters represent different groups based on Tukey's HSD test (adjusted $P < 0.05$)

(See figure on next page.)

Fig. 6 Infection of $\Delta Cfhos2$ mutant elicits stronger plant defense reactions. Infected apple leaves were sampled at 2–4 days post-inoculation (dpi). Fungal infectious hyphae were visualized with the aid of FITC-WGA staining. **a** At the early infection phase, WT differentiates elongated invasive hyphae (left) whereas $\Delta Cfhos2$ ($\Delta hos2-4$) differentiates spherical vesicles with distorted branches (right), the mutant also elicits cytoplasmic condensation or browning of apple epidermal cells (rightmost). **b** Infectious hyphae of $\Delta Cfhos2$ ($\Delta hos2-4$) induces stronger degree of mesophyll cell browning than WT (1104-6). **c** Distortion of infectious hyphae of the $\Delta Cfhos2$ ($\Delta hos2-4$) mutant. Scale bars in **a** and **c** represent 20 μm , scale bars in **b** represent 50 μm

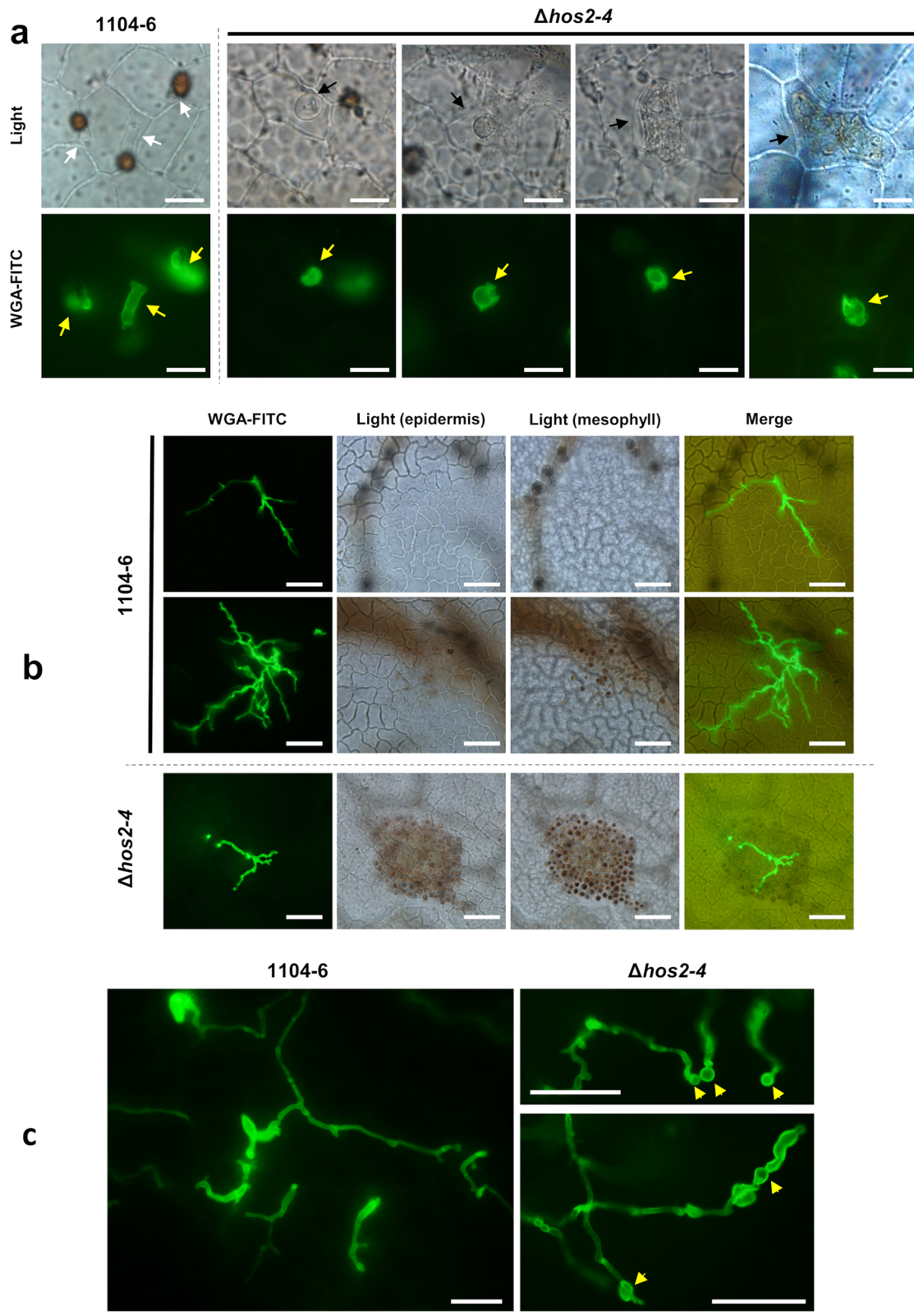


Fig. 6 (See legend on previous page.)

penetration sites of epidermal cells, 1104-6 formed normally branched and elongated infectious hyphae (Fig. 6a, left); $\Delta hos2-4$, on the other hand, produced spherical vesicles, with only thin, short, and distorted hyphal branches extending outward on the vesicle surface (Fig. 6a, right). These mutant vesicles appeared to be intracellular, and the associated host epidermal cells accumulated defense reactions manifested by cytoplasm shrinkage, granulation, or even browning (Fig. 6a). $\Delta hos2-4$ could also form elongated mycelia, which however, were associated with intense browning reactions of the underneath mesophyll cells (Fig. 6b). In rare cases, $\Delta hos2-4$ produced long invasive hyphae (>200 μm in length). The tips of these hyphae, however, were frequently distorted, manifested by bulbous extrusions (Fig. 6c). The results demonstrated that $\Delta hos2-4$ infection elicits stronger plant defense reactions than its WT parent.

Transcriptome comparison between WT and $\Delta hos2-4$ infections at the early infection phase

To dissect the impact of *Cfhos2* deletion on plant–pathogen interactions in more detail, we performed dual plant–pathogen transcriptome comparison between WT and $\Delta hos2-4$ infections at their early infection phase (36 hours post-inoculation, hpi). Three biological replicates of apple leaf tissues infected with 1104-6 or $\Delta hos2-4$ were sequenced. For each replicate, around 6 Gb clean pair-reads (150 bp in length) were generated. Concordant reads pairs being mapped to apple reference genome ranged between 15.3 million and 19.6 million (~77% in percentage) whereas those being mapped to *C. fructicola* reference genome ranged between 0.03 million and 0.08 million (0.1–0.3% in percentage), and reads mapping results for individual libraries were summarized in Additional file 2: Table S2.

Apple leaf tissues inoculated with WT or $\Delta hos2-4$ were highly similar in transcriptome pattern. Based on EdgeR analysis (Additional file 1: Figure S4a and Additional file 3: Table S3), merely 67 genes were identified as differentially expressed genes (DEGs, relative fold change >2, FDR < 0.05), of which 62 showed lower expressions in tissues infected by $\Delta hos2-4$. These 67 DEGs are functionally related to plant cell wall degradation or modification (e.g., pectinases, glucanases, extensins, 9 genes in total), stress responses (e.g., peroxidases, lipid-transfer proteins, heat shock proteins, 13 genes in total), defense signaling (e.g., LRR receptor-like kinase, wall-associated receptor kinase, L-type lectin, 3 genes in total), secondary metabolism (e.g., chalcone synthase, 4-hydroxycoumarin synthase, cytochrome P450, 6 genes in total), as well as metal binding (e.g., cupredoxins, metallothioneins, 5 genes in total). The up-regulated genes related to cell wall degradation, stress response, and defense signaling during WT

infection might be related to the stronger colonization activities of the strain. Only five DEGs showed higher expression in $\Delta hos2-4$ -infected than in WT-infected leaf tissues, among which *LOC103456334* encodes an F-box protein similar (33% amino acid identity) to the immunity regulator CPR30 in *Arabidopsis* (constitutive expresser of PR genes 30, *AT4G12560*; Gou et al. 2009, 2012), and *LOC103428825* encodes a small protein similar (72% amino acid identity) to *Arabidopsis* FPF1 (*AT5G24860*) that regulates flowering and gibberellin signaling (Kania et al. 1997).

We further validated the expressions of eight putative infection-related genes by reverse transcription-quantitative PCR (RT-qPCR) (Fig. 7), and the results confirmed down-regulation of the genes encoding xyloglucan endotransglucosylase (*LOC103423907*), metallothionein (*LOC103447702*), and 4-hydroxycoumarin synthase (*LOC103456250*) in $\Delta hos2-4$ -infected apple leaf tissues relative to WT-infected tissues. These genes are functionally related to plant cell wall hydrolysis, metal binding, and secondary metabolism. Several defense marker genes, including *WRKY29* (*LOC103439197*), *MAPKKK17-like* (*LOC103416013*), and *CAS2* (callose synthase 2-like gene, *LOC103438357*), were similarly expressed between WT- and $\Delta hos2-4$ -infected leaf tissues. In contrast, *LOC103456334*, an *Arabidopsis* CPR30 homologous gene, was significantly up-regulated in response to $\Delta hos2-4$ infection. The expression level of this gene in $\Delta hos2-4$ -infected apple tissues was 67-fold higher than that in WT-infected tissues at 24 hpi, but was similar to that of WT at 48 hpi. *LOC103412892* and *LOC108171028* encode two putative R proteins, a RGA3-like LRR protein and a RPP13-like CC-NB-ARC protein, respectively. RNA-seq supported their slightly higher expression in $\Delta hos2-4$ -infected tissues (close to twofold up-regulation), however RT-qPCR supported their similar expression levels between WT- and $\Delta hos2-4$ -infected samples (Fig. 7).

In identifying fungal DEGs, we pre-filtered lowly expressed genes with a stringent counts per million (CPM) threshold (<30 in at least three samples) given the apparent low ratio of fungal reads in the RNA-seq sample, and such pre-filtering should reduce the potential noisy effect associated with the CPM discreteness. In total, 291 fungal DEGs were identified (relative fold change >2, FDR < 0.05) between WT and $\Delta hos2-4$, among which 193 were up-regulated and 98 were down-regulated in $\Delta hos2-4$ (Additional file 1: Figure S4b and Additional file 3: Table S4). PFAM enrichment analysis (Additional file 1: Figure S4c) showed that the genes up-regulated in $\Delta hos2-4$ were functionally relevant to plant surface attachment (PF11327, egh16-like virulence factor; PF12296, hydrophobic surface binding protein A), secondary

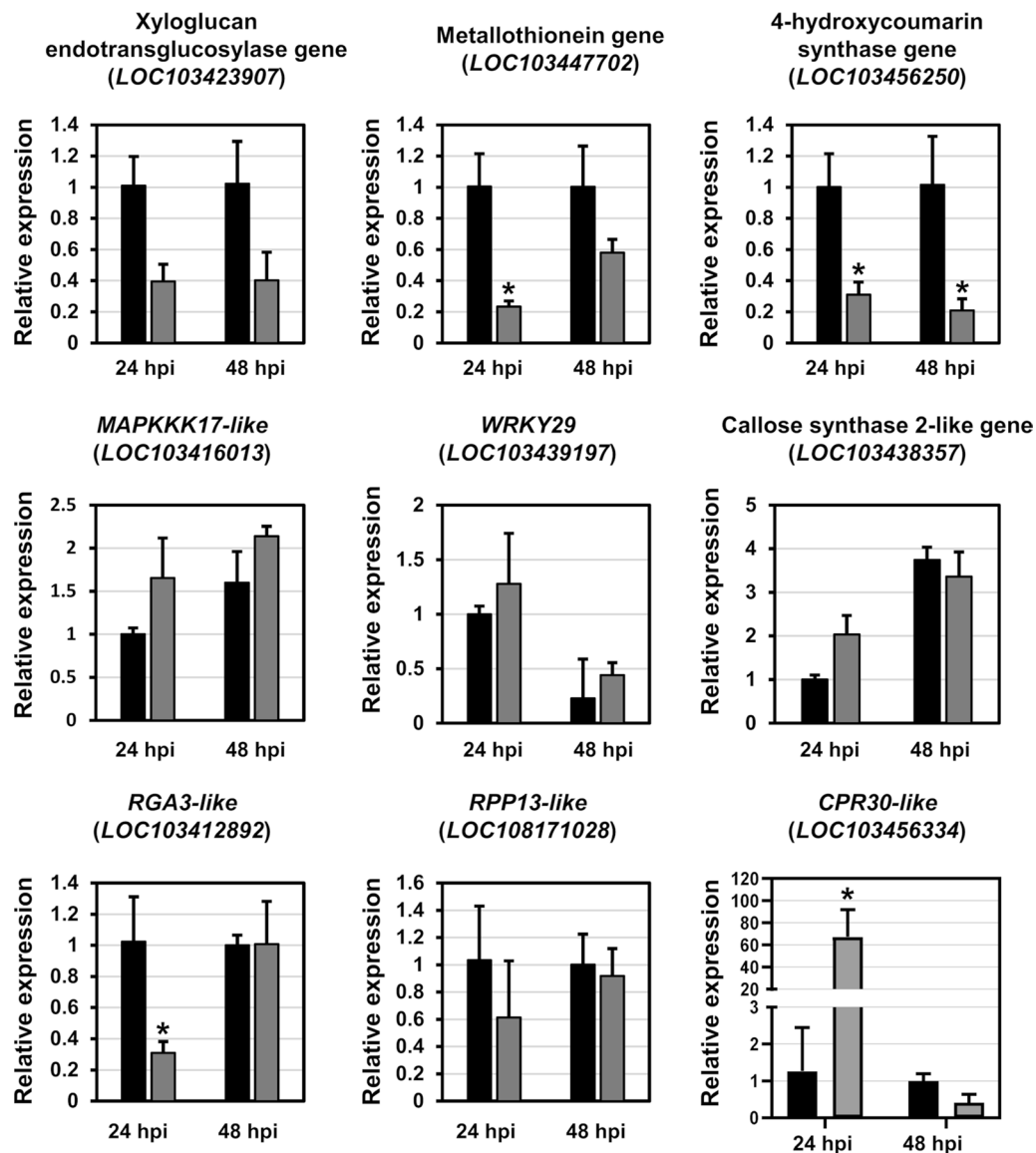


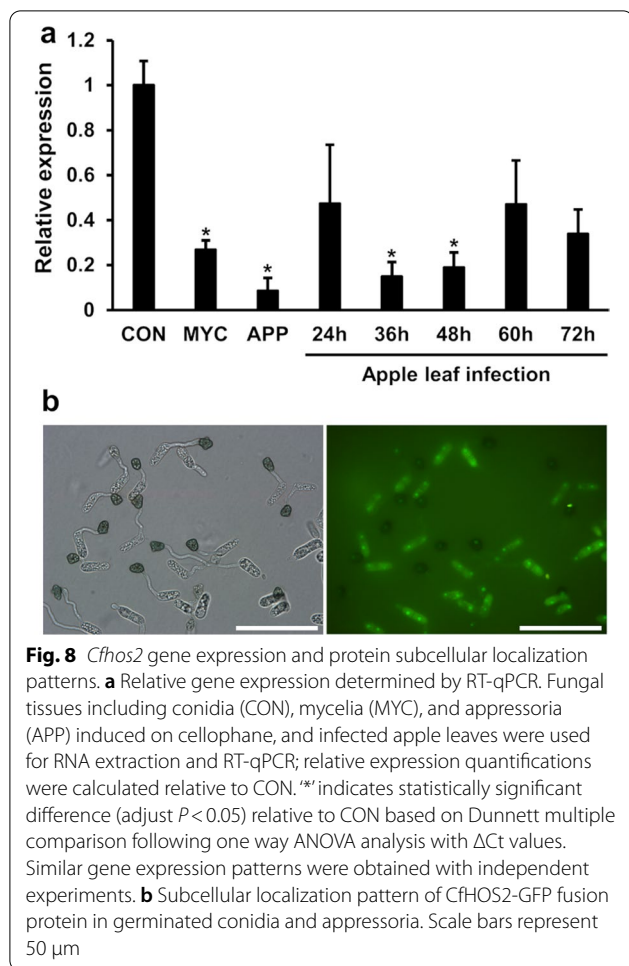
Fig. 7 Expression of apple defense-related genes in response to inoculation with WT (1104-6) (black bar) or Δ hos2-4 mutant (grey bar) at 24 and 48 hours post-inoculation (hpi). Expressions were determined by RT-qPCR, and relative expression values were calculated relative to WT at 24 hpi. Error bar indicates standard deviation based on three independent technical replicates, and "*" indicates statistically significant difference ($P < 0.05$) relative to WT at the corresponding time point based on two-tailed t -test with Δ Ct values. Similar gene expression patterns were obtained with independent experiments

metabolism (PF00005, ABC transporter; PF01565, FAD binding; PF00067, cytochrome P450; PF00501, AMP-binding enzyme), and kinase signaling (PF00069, protein kinase). On the other hand, genes related to amino acid metabolism (PF02729, aspartate/ornithine carbamoyl-transferase) and CFEM (PF05730) were enriched among genes being down-regulated in Δ hos2-4. The 291 DEGs also contained 10 small secreted protein genes (SSPs, containing predicted secretory peptide, lacking transmembrane domain, amino acid length < 300), eight of

which were up-regulated in Δ hos2-4. Enrichment of SSPs among DEGs, however, was not statistically significant based on hypergeometric test (data not shown).

Gene expression profile and subcellular localization of *Cfhos2*

RT-qPCR was performed to determine the expression levels of *Cfhos2* in conidia, vegetative mycelia, and appressoria of *C. fructicola*, and in apple leaves at different time points after infection with *C. fructicola* (Fig. 8a).



Highest gene expression level was observed in conidia. Relative to that in conidia, the gene expression level was 3.7-fold lower in mycelia, 11.7-fold lower in appressoria, and 2.1–6.7-fold lower during infection of apple leaves. Consistent with the gene expression data, GFP fluorescence signal of the *hos2-4-3* strain (expressing HOS2-GFP fusion protein under the native promoter of *Cfhos2*) was strong in conidia and germinated conidia, but weak in vegetative hyphae (data not shown). The subcellular distribution pattern of GFP fluorescence was in accordance with a nucleus protein localization (Fig. 8b).

Discussion

Colletotrichum species employ a complex two-stage strategy called 'hemibiotrophy' to infect host plants. Generally, successful pathogen infection requires sequential development of infection structures and dynamic expression of various virulence factors such as effectors, secondary metabolites, and plant cell wall-degrading enzymes. *Colletotrichum* pathogens are thus suggested to possess delicate mechanisms to sense

various environmental signals and regulate transcription (Kleemann et al. 2012; O'Connell et al. 2012). Histone modifications, such as acetylation, methylation, and phosphorylation, are important epigenetic mechanisms regulating eukaryotic gene expression. So far, however, information regarding the roles of histone modification enzymes in *Colletotrichum* pathogenesis remains limited. In particular, no *Colletotrichum* HDAC has been functionally characterized except for HOS2 in *C. gloeosporioides* (Liu et al. 2022). In this study, we characterized four class I HDACs in *C. fructicola* and dissected the virulence functions of *Cfhos2* in detail. Our study results provide important insights into the virulence mechanisms of *C. fructicola*, and likely other phytopathogens as well.

The results of targeted gene deletion supported that the four characterized class I HDACs perform different functions in *C. fructicola*, and the functional specialization pattern appears conserved among filamentous ascomycetes. First, our repeated attempt to delete *Cfrpd3* gene failed, indicating a lethal effect or a severe growth defect for the mutant. Such result is in accordance with the report that deletion of *rpd3* in filamentous ascomycetes is either lethal (e.g., *A. nidulans*, *A. fumigatus*, *Botrytis cinerea*, and *M. oryzae*) or causes severe growth defect (e.g., *B. bassiana* and *F. graminearum*) (Lai et al. 2022). Second, deletion of *Cfhos3* or *Cfhda1* had no obvious effect on fungal growth, virulence, and stress tolerances, which is consistent with a recent study reporting that *hos3* or *hda1* gene deletion in *Alternaria alternata* does not affect fungal radial growth, conidiation, virulence, carbon source utilization, and stress tolerances (Ma et al. 2021). Third, in accordance with our study result that *Cfhos2* is pivotal for successful GLS pathogenesis in *C. fructicola*, Set3C/Hos2 complex is conservatively required for full virulence of various plant and human fungal pathogens (Lai et al. 2022). In sum, our study results corroborate the conserved requirement of *rpd3* for vegetative growth and the conserved requirement of *hos2* for pathogenesis, respectively, among filamentous ascomycetes.

Disruption of *Cfhos2* in *C. fructicola* had mild impact on fungal vegetative growth, but led to severe virulence defect toward apple leaf tissue. *Cfhos2* deletion mutants were almost non-pathogenic in both unwounded and wounded inoculations, supporting a virulence function of *Cfhos2* at the post-invasive phase. Such results differ from the study with *C. gloeosporioides*, in which pre-wounding of leaf tissue fully restored the virulence defect of the mutant, indicating fine-tuned functional diversification of *hos2* gene among *Colletotrichum* lineages (Liu et al. 2022). In our histological observation, $\Delta Cfhos2$ mutant infection elicited distortion of fungal invasive hyphae and browning and granulation of host epidermal

cells, we postulated a failure of the mutant in activating plant defense-suppressors (e.g., effectors and secondary metabolites), or in repressing the release of plant defense elicitors. Our RNA-sequencing experiment showed that $\Delta Cfhos2$ infection induces the up-regulation of genes related to secondary metabolism (e.g., NADH oxidoreductases, ABC transporters, AMP binding enzymes, and cytochrome P450s), implying the importance of secondary metabolites in manipulating plant defenses. *Colletotrichum* genomes are rich in secondary metabolite biosynthetic genes (O'Connell et al. 2012; Liang et al. 2018b); moreover, various *Colletotrichum* secondary metabolites, such as phenoxyacetic acid, indoleacetic acid, mycosporine alanine, diketopiperazine, ferricrocin, and cercosporin, have phytotoxic activities (García-Pajón and Collado 2003; de Jonge et al. 2018; Dallery et al. 2019).

Compared with WT, the $\Delta Cfhos2$ mutants were hypersensitive to the cell wall stress-eliciting compound CR. During infection, infectious hyphae of the mutant were frequently distorted. Such results suggest that *Cfhos2* deletion might affect cell wall integrity, rendering the mutant more susceptible to plant defenses. In addition to its protective function, fungal cell wall is an important source of immunity-triggering elicitors (e.g., chitin and β -glucan fragments) (Gow et al. 2017). During infection, *Colletotrichum* pathogens can actively modify the cell wall layer to evade plant host detection or attenuate defense elicitation (Oliveira Silva et al. 2022). In this regard, a dysfunctional cell wall layer may render the $\Delta Cfhos2$ mutants more vulnerable to plant defenses.

Appressorium is an important infection structure mediating plant penetration. In this study, *Cfhos2* deletion did not affect conidial yield and germination, but severely reduced appressorium differentiation and appressorium-mediated penetration on cellophane membrane. Fungal HOS2 regulates many developmental processes including asexual and sexual developments (Ding et al. 2010; Li et al. 2011; Cai et al. 2018), conidium and colony morphology (Baidyaroy et al. 2001; Liu et al. 2022), and yeast-to-filament transition (Hnisz et al. 2010; Elías-Villalobos et al. 2015). However, the involvement of HOS2 in regulating appressorium development has so far only been reported in *C. gloeosporioides* (Liu et al. 2022). In *Cochliobolus carbonum* and *M. oryzae*, *hos2* deletion does not affect appressorium development, but affects appressorium-mediated plant penetration (Baidyaroy et al. 2001; Ding et al. 2010). Interestingly, in contrast with its defect on cellophane membrane, *Cfhos2* deletion mutants differentiated appressorium normally on parafilm and apple leaf surface, supporting that *Cfhos2* regulates appressorium development in a surface-dependent manner, for which we propose two potential mechanisms.

First, hydrophobicity and wax signals may independently regulate appressorium development, and only the former signal requires *Cfhos2*. In fungi, multiple environmental signals can trigger appressorium development, and these signals can even function through independent genetic pathways. For instance, double deletion mutants of *Mosho1* and *Momsb2* in *M. oryzae* fail to perceive hydrophobicity signal for appressorium differentiation, but the mutants are fully responsive to epicuticular leaf wax stimuli (Liu et al. 2011). Parafilm and apple leaf cuticle are rich in wax that can trigger *Colletotrichum* appressorium development (Podila et al. 1993). The presence of such wax signal may bypass the deficiency of *Cfhos2* deletion mutants in response to hydrophobicity surface signal. Otherwise, *Cfhos2* may be important for sensing both wax and hydrophobicity signals, but parafilm and apple leaf surfaces enable more robust signal transduction due to their elevated hydrophobicity and more waxy property. Fungal histone modification enzymes can fine-tune the kinetics of gene transcriptional induction, enabling more stringent control of signaling and development (Hnisz et al. 2010). *Cfhos2* may function as a signal enhancer in this regard, where a stronger upstream signal compensates for the mutant deficiency in activating downstream gene expression and development.

While our research data demonstrated the critical virulence functions of *Cfhos2*, its downstream target genes are still unclear. ChIP analyses in other fungal organisms highlight the regulatory effects of fungal HOS2 on genes related to cAMP-PKA signaling, pheromone responses, autophagic homeostasis, and secondary metabolite biosynthesis (Hnisz et al. 2010; Elías-Villalobos et al. 2015; He et al. 2018; Lan et al. 2019). A recent transcriptome study in *A. alternata* also highlights the function of HOS2 as a global transcriptional regulator (Ma et al. 2021). So far, however, many of these transcriptomic studies have been performed with in vitro fungal tissues, and the potential virulence-related targets in planta have not been characterized. In this study, we performed a transcriptome comparison between WT and $\Delta Cfhos2$ at the early infection phase and identified 291 fungal DEGs. It is interesting that many of these genes are functionally related to pathogenesis (e.g., functions related plant surface attachment, secondary metabolism, kinase signaling, CFEM proteins, and SSPs); more importantly, secondary metabolism and SSPs are categories being highly enriched among infection-specific genes in our previous study (Liang et al. 2018a). Such result highlights the potential involvement of *Cfhos2* in regulating the expression of virulence genes. We also examined the influence of *Cfhos2* deletion on plant gene expression. Whereas many defense genes were similarly expressed in response to infections by WT and $\Delta Cfhos2$, a defense related F-box

gene (*LOC103456334*) was strongly up-regulated by infection with $\Delta Cfhos2$ at 24 hpi. The gene is homologous to *CPR30* from *Arabidopsis*, which functions as a negative regulator of both SA-dependent and SA-independent defense signaling (Gou et al. 2009, 2012). The potential immune function of this gene awaits further experimental validation.

Conclusions

Based on phenotypic characterization of gene deletion mutants, we demonstrated that *Cfhos2* is a key epigenetic factor regulating growth, stress tolerance, appressorium development, and plant defense suppression in the GLS pathogen *C. fructicola*. Our results highlight the important contribution of histone acetylation modification toward GLS pathogenesis, and provide insights into the potential mechanisms underlying this regulation.

Methods

Fungal strains, culture conditions, and nucleic acid manipulations

The *C. fructicola* 1104-6 strain was used as WT strain. WT and its derivative mutant strains were all maintained on PDA and preserved as glycerol stock (15%) at -80°C . Genomic DNA extraction from mycelia was performed with a modified cetyl trimethylammonium bromide (CTAB) procedure (Allen et al. 2006). Total RNA was extracted with a RNAsimple Kit (TIANGEN, DP419, Beijing, China). RT-qPCR was performed in the same way as previously described (Liang et al. 2018a). DNA cloning and subcloning were performed with a recombinase-based cloning kit (TRANSGEN, CU201-02). The primers used in this study are listed in Additional file 4: Table S5.

Bioinformatic analysis, gene deletion, and complementation

Putative HDACs encoded by the *C. fructicola* genome were identified by BlastP search against the *C. fructicola* 1104-7 genome (Liang et al. 2018b) using AnHosA from *A. nidulans* (GenBank accession: CBF75342) as a protein query (Pidroni et al. 2018). For phylogenetic analysis, functionally characterized fungal HDACs were retrieved from GenBank, and sequence alignment and phylogenetic tree construction were performed with MEGA 7.0. Putative protein domains were identified by Interproscan. To generate gene deletion mutants, overlap PCR was performed to generate gene deletion construct, which was transformed into protoplast based on a described procedure (Liang et al. 2019). Gene deletion mutants were identified based on hygromycin resistance (100 $\mu\text{g}/\text{mL}$) selection, PCR screening, and Southern blot analysis. For genetic complementation of the *Cfhos2*-deleted mutant $\Delta hos2-4$, a 3611 bp DNA fragment encompassing the

coding region of *Cfhos2* and 2126 bp of the 5' upstream region was amplified using total genomic DNA as the template, the PCR fragment was then cloned into the *EcoRI* restriction site of pHZ100-GFP (Liang et al. 2019). The obtained construct pHZ100-HOS2-GFP allowed for C-terminal GFP fusion expression under the native gene promoter of *Cfhos2*. The vector was transformed into $\Delta hos2-4$ after sequencing verification. Complementation strains were identified based on G418 resistance (300 $\mu\text{g}/\text{mL}$), GFP fluorescence, and phenotypic complementation phenotypes.

Phenotypic characterization

Fungal strains were cultured on PDA medium to examine colony morphology and to measure radial growth rate. Conidial production was incubated with shaking in PDB as previously described (Wang et al. 2017). Appressorium formation and penetration assays were performed by inoculating conidial suspension on cellophane surface; 200 μL conidial suspension (5×10^6 conidia/mL) was spread on cellophane overlaid agar medium (2% agar). After incubation at room temperature for 10–18 h, conidial germination, appressorium differentiation, and infectious hyphae development were examined under light microscope.

To test the impact of *Cfhos2* deletion on stress tolerance of *C. fructicola*, fungal strains were incubated on PDA supplemented with different stress agents (1.0 M NaCl, 1.0 M KCl, or 1.0 M sorbitol was used to mimic osmotic stress; 10 mM H_2O_2 , 0.2% SDS, and 500 $\mu\text{g}/\text{mL}$ CR were used to mimic oxidative, membrane damage, and cell wall stresses, respectively). PDA buffered at pH 3.0 and pH 8.0 were used to test acidic and alkaline stresses (Liang et al. 2019). To investigate the role of *Cfhos2* in nutrient utilization, the tested strains were cultured on MM, pectin, and carboxymethyl cellulose (CMC) plates. For pectin and CMC plates, glucose was substituted by 0.5% of pectin and CMC, respectively.

To investigate the pathogenic functions of *Cfhos2*, freshly harvested Gala apple leaves or fruits were spray-inoculated with conidial suspensions (1×10^7 conidia/mL) of the tested fungal strains and kept inside a moisture chamber until symptom appeared. Leaves were sampled at different time points post-inoculation for histological observation. Sampled leaves were surface-sterilized as previously described (Liang et al. 2019) and stained with trypan blue or FITC-WGA prior to observation under light or fluorescent microscope. Virulence assay on pear fruit was performed with fruits bought from local grocery store. Pear fruits were surface-sterilized with 70% alcohol, pre-wounded with pin-hole needles and inoculated with mycelial plugs. Inoculated fruits

were kept in a moisture chamber at room temperature for disease development.

RNA sequencing analysis and RT-qPCR

To gain deeper insights into the involvement of *Cfhos2* in regulating plant–pathogen interactions, we compared transcriptome differences between apple leaf tissues inoculated with WT and Δ *hos2-4* by RNA-sequencing. Infected apple leaves were sampled at 36 hpi, a time point corresponding to pathogen penetration and initial invasive hyphae development. Three biological replicates were sequenced for both 1104-6 and Δ *hos2-4*. For each replicate, around 6 Gb clean pair-reads (150 bp in length) were generated, which were mapped against a locally assembled *C. fructicola* 1104-7 reference genome and the ‘Golden Delicious’ apple reference genome GDDH13 Version 1.1 (<https://iris.angers.inra.fr/gddh13/>) using TopHat version 2.1.0 (Kim et al. 2013). Read counts for each gene model were retrieved with HTSeq version 0.6.0 (Anders et al. 2015). DEGs were identified based on EdgeR package (Anders et al. 2015). Normalized CPM values were used to calculate relative fold changes (FCs), and DEGs were defined as genes with $|\log_2FC| > 1$ and adjusted *P* value (padj) < 0.05 . Functional enrichment tests of PFAM domains were performed with FunRich version 2.1.2 (Pathan et al. 2015). The complete transcriptome data sets are available at the Gene Expression Omnibus at the National Center for Biotechnology Information (NCBI) under the accession number PRJNA857179. RT-qPCR was performed to validate RNA-seq gene expressions based on a previously described procedure (Liang et al. 2018a), and total RNAs extracted from different tissues were used for reverse transcription. The apple *actin-7* gene (*LOC103453508*) was chosen as the internal reference gene for quantifying the expression of apple genes, and relative quantifications were performed with a delta delta Ct approach. To determine the expression dynamics of *Cfhos2* gene, fungal tissues including conidia (collected from PDB shake culture for 4 days), mycelia (collected from PDB shake culture for 2 days after conidial inoculation), appressoria (induced on cellophane membrane surface), and infected apple tissues at different time points were collected for total RNA extraction and RT-qPCR analysis, and the *C. fructicola* β -*tubulin* gene (Liang et al. 2018a) was used as the internal reference control.

Abbreviations

ChIP-seq: Chromatin immunoprecipitation followed by sequencing; CMC: Carboxymethyl cellulose; CPM: Counts per million; CR: Congo red; DEGs: Differently expressed genes; dpi: Days post-inoculation; FITC-WGA: Fluorescein isothiocyanate-conjugated WGA; FDR: False discovery rate; GLS: Glomerella leaf spot; HDAC: Histone deacetylase; hpi: Hours post-inoculation; MM:

Minimum (nutrient poor) medium; TSA: Trichostatin A; WGA: Wheat germ agglutinin; WT: Wild type.

Supplementary Information

The online version contains supplementary material available at <https://doi.org/10.1186/s42483-022-00144-y>.

Additional file 1: Figure S1. Southern blot and PCR detection of *Cfhos2* deletion mutants. **Figure S2.** Gene deletion mutants of *Cfhos3* and *Cfhd1* exhibit normal phenotypes in vegetative growth rate, sensitivity to trichostatin A (TSA), and pathogenicity. **Figure S3.** Deletion of *Cfhos3* or *Cfhd1* does not affect stress tolerance and appressorium development of *Colletotrichum fructicola*. **Figure S4.** Identification of differently expressed gene (DEGs) between WT (1104-6) and *Cfhos2* deletion mutant (Δ *hos2-4*) in both apple leaves and *Colletotrichum fructicola* at the early infection phase (36 hpi).

Additional file 2: Table S1. Variation in growth inhibition of different strains under the indicated stress agents. **Table S2.** Summary statistics of reads mapping outcomes for individual RNA-seq libraries against the *Colletotrichum fructicola* and apple (*Malus domestica*) reference genomes.

Additional file 3: Table S3. DEGs identified in apple leaves infected with the *Colletotrichum fructicola* wild-type strain or *Cfhos2* deletion mutant at the early infection phase (36 hpi). **Table S4.** DEGs identified between the *Colletotrichum fructicola* wild-type strain and *Cfhos2* deletion mutant at the early infection phase (36 hpi).

Additional file 4: Table S5. Primers used in this study.

Acknowledgements

Not applicable.

Author contributions

XL, RZ, and GS conceived and designed the study. MC, ZZ, HT, WY (Wei Yu), XZ, and WY (Wenrui Yang) performed the experiments. XL and MC analyzed the data and drafted the manuscript. XL, RZ, and GS revised the manuscript and supervised the research. All authors read and approved the final manuscript.

Funding

This research was funded by the National Natural Science Foundation of China (32072374, 32070144), the Natural Science Foundation of Shaanxi (2020JQ-255), and China Agriculture Research System of MOF and MARA (CARS27).

Availability of data and materials

The datasets generated and/or analysed during the current study are available in NCBI repository, <https://www.ncbi.nlm.nih.gov/bioproject/PRJNA857179>.

Declarations

Ethics approval and consent to participate

Not applicable.

Consent for publication

Not applicable.

Competing interests

The authors declare that they have no competing interests.

Received: 14 July 2022 Accepted: 10 October 2022

Published online: 24 October 2022

References

Allen GC, Flores-Vergara MA, Krasynanski S, Kumar S, Thompson WF. A modified protocol for rapid DNA isolation from plant tissues using

- cetyltrimethylammonium bromide. *Nat Protoc.* 2006;1(5):2320–5. <https://doi.org/10.1038/nprot.2006.384>.
- Anders S, Pyl PT, Huber W. HTSeq—a Python framework to work with high-throughput sequencing data. *Bioinformatics.* 2015;31(2):166–9. <https://doi.org/10.1093/bioinformatics/btu638>.
- Baidyaroy D, Brosch G, Ahn JH, Graessle S, Wegener S, Tonukari NJ, et al. A gene related to yeast *HOS2* histone deacetylase affects extracellular depolymerase expression and virulence in a plant pathogenic fungus. *Plant Cell.* 2001;13(7):1609–24. <https://doi.org/10.1105/TPC.010168>.
- Bannister AJ, Kouzarides T. Regulation of chromatin by histone modifications. *Cell Res.* 2011;21(3):381–95. <https://doi.org/10.1038/cr.2011.22>.
- Cai Q, Tong S, Shao W, Ying S, Feng M. Pleiotropic effects of the histone deacetylase Hos2 linked to H4–K16 deacetylation, H3–K56 acetylation, and H2A–S129 phosphorylation in *Beauveria bassiana*. *Cell Microbiol.* 2018;20(7): e12839. <https://doi.org/10.1111/cmi.12839>.
- Dallery JF, Adelin É, Le Goff G, Pigné S, Auger A, Ouazzani J, et al. H3K4 trimethylation by CclA regulates pathogenicity and the production of three families of terpenoid secondary metabolites in *Colletotrichum higginsianum*. *Mol Plant Pathol.* 2019;20(6):831–42. <https://doi.org/10.1111/mpp.12795>.
- de Jonge R, Ebert MK, Huitt-Roehl CR, Pal P, Suttle JC, Spanner RE, et al. Gene cluster conservation provides insight into cercosporin biosynthesis and extends production to the genus *Colletotrichum*. *Proc Natl Acad Sci USA.* 2018;115(24):E5459–66. <https://doi.org/10.1073/pnas.1712798115>.
- Ding S, Liu W, Iliuk A, Ribot C, Vallet J, Tao A, et al. The tig1 histone deacetylase complex regulates infectious growth in the rice blast fungus *Magnaporthe oryzae*. *Plant Cell.* 2010;22(7):2495–508. <https://doi.org/10.1105/tpc.110.074302>.
- Dubey A, Jeon J. Epigenetic regulation of development and pathogenesis in fungal plant pathogens. *Mol Plant Pathol.* 2017;18(6):887–98. <https://doi.org/10.1111/mpp.12499>.
- Elías-Villalobos A, Fernández-Álvarez A, Moreno-Sánchez I, Helmlinger D, Ibeas JI. The Hos2 histone deacetylase controls *Ustilago maydis* virulence through direct regulation of mating-type genes. *PLoS Pathog.* 2015;11(8): e1005134. <https://doi.org/10.1371/journal.ppat.1005134>.
- García-Pajón CM, Collado IG. Secondary metabolites isolated from *Colletotrichum* species. *Nat Prod Rep.* 2003;20(4):426–31. <https://doi.org/10.1039/B302183C>.
- Gonçalves AE, Velho AC, Stadnik MJ. Formation of conidial anastomosis tubes and melanization of appressoria are antagonistic processes in *Colletotrichum* spp. from apple. *Eur J Plant Pathol.* 2016;146(3):497–506. <https://doi.org/10.1007/s10658-016-0934-6>.
- Gou M, Su N, Zheng J, Huai J, Wu G, Zhao J, et al. An F-box gene, *CPR30*, functions as a negative regulator of the defense response in *Arabidopsis*. *Plant J.* 2009;60(5):757–70. <https://doi.org/10.1111/j.1365-3113.2009.03995.x>.
- Gou M, Shi Z, Zhu Y, Bao Z, Wang G, Hua J. The F-box protein CPR1/CPR30 negatively regulates R protein SNC1 accumulation. *Plant J.* 2012;69(3):411–20. <https://doi.org/10.1111/j.1365-3113.2011.04799.x>.
- Gow NAR, Latge JP, Munro CA. The fungal cell wall: structure, biosynthesis, and function. *Microbiol Spectr.* 2017. <https://doi.org/10.1128/microbiolspec.FUNK-0035-2016>.
- Hamada NA, Moreira RR, Nesi CN, May De Mio LL. Pathogen dispersal and Glomerella leaf spot progress within apple canopy in Brazil. *Plant Dis.* 2019;103(12):3209–17. <https://doi.org/10.1094/PDIS-08-18-1375-RE>.
- He M, Xu Y, Chen J, Luo Y, Lv Y, Su J, et al. MoSnt2-dependent deacetylation of histone H3 mediates MoTor-dependent autophagy and plant infection by the rice blast fungus *Magnaporthe oryzae*. *Autophagy.* 2018;14(9):1543–61. <https://doi.org/10.1080/15548627.2018.1458171>.
- Hnisz D, Majer O, Frohner IE, Komnenovic V, Kuchler K. The Set3/Hos2 histone deacetylase complex attenuates cAMP/PKA signaling to regulate morphogenesis and virulence of *Candida albicans*. *PLoS Pathog.* 2010;6(5): e1000889. <https://doi.org/10.1371/journal.ppat.1000889>.
- Hnisz D, Bardet AF, Nobile CJ, Petryshyn A, Glaser W, Schöck U, et al. A histone deacetylase adjusts transcription kinetics at coding sequences during *Candida albicans* morphogenesis. *PLoS Genet.* 2012;8(12): e1003118. <https://doi.org/10.1371/journal.pgen.1003118>.
- Jeon J, Kwon S, Lee YH. Histone acetylation in fungal pathogens of plants. *Plant Pathol J.* 2014;30(1):1–9. <https://doi.org/10.5423/PPJ.RW.01.2014.0003>.
- Kania T, Russenberger D, Peng S, Apel K, Melzer S. PPF1 promotes flowering in *Arabidopsis*. *Plant Cell.* 1997;9(8):1327–38. <https://doi.org/10.1105/tpc.9.8.1327>.
- Kim D, Perte G, Trapnell C, Pimentel H, Kelley R, Salzberg SL. TopHat2: accurate alignment of transcriptomes in the presence of insertions, deletions and gene fusions. *Genome Biol.* 2013;14(4):R36. <https://doi.org/10.1186/gb-2013-14-4-r36>.
- Kleemann J, Rincon-Rivera LJ, Takahara H, Neumann U, Ver Loren van Themaat E, van der Does HC, et al. Sequential delivery of host-induced virulence effectors by appressoria and intracellular hyphae of the phytopathogen *Colletotrichum higginsianum*. *PLoS Pathog.* 2012;8(4):e1002643. <https://doi.org/10.1371/journal.ppat.1002643>.
- Kurdistani SK, Grunstein M. Histone acetylation and deacetylation in yeast. *Nat Rev Mol Cell Biol.* 2003;4(4):276–84. <https://doi.org/10.1038/nrm1075>.
- Lai Y, Wang L, Zheng W, Wang S. Regulatory roles of histone modifications in filamentous fungal pathogens. *J Fungi.* 2022;8(6):565. <https://doi.org/10.3390/jof8060565>.
- Lan H, Wu L, Sun R, Keller NP, Yang K, Ye L, et al. The HosA histone deacetylase regulates aflatoxin biosynthesis through direct regulation of aflatoxin cluster genes. *Mol Plant Microbe Interact.* 2019;32(9):1210–28. <https://doi.org/10.1094/MPMI-01-19-0033-R>.
- Li Y, Wang C, Liu W, Wang G, Kang Z, Kistler HC, et al. The *HDF1* histone deacetylase gene is important for conidiation, sexual reproduction, and pathogenesis in *Fusarium graminearum*. *Mol Plant Microbe Interact.* 2011;24(4):487–96. <https://doi.org/10.1094/MPMI-10-10-0233>.
- Liang X, Shang S, Dong Q, Wang B, Zhang R, Gleason ML, et al. Transcriptomic analysis reveals candidate genes regulating development and host interactions of *Colletotrichum fructicola*. *BMC Genom.* 2018a;19(1):557. <https://doi.org/10.1186/s12864-018-4934-0>.
- Liang X, Wang B, Dong Q, Li L, Rollins JA, Zhang R, et al. Pathogenic adaptations of *Colletotrichum* fungi revealed by genome wide gene family evolutionary analyses. *PLoS ONE.* 2018b;13(4): e0196303. <https://doi.org/10.1371/journal.pone.0196303>.
- Liang X, Wei T, Cao M, Zhang X, Liu W, Kong Y, et al. The MAP kinase CfPMK1 is a key regulator of pathogenesis, development, and stress tolerance of *Colletotrichum fructicola*. *Front Microbiol.* 2019;10:1070. <https://doi.org/10.3389/fmicb.2019.01070>.
- Liang X, Yao L, Hao X, Li B, Kong Y, Lin Y, et al. Molecular dissection of perithecial mating line development in *Colletotrichum fructicola*, a species with a nontypical mating system featuring plus-to-minus switch and plus-minus-mediated sexual enhancement. *Appl Environ Microbiol.* 2021;87(12): e0047421. <https://doi.org/10.1128/AEM.00474-21>.
- Liu W, Zhou X, Li G, Li L, Kong L, Wang C, et al. Multiple plant surface signals are sensed by different mechanisms in the rice blast fungus for appressorium formation. *PLoS Pathog.* 2011;7(1): e1001261. <https://doi.org/10.1371/journal.ppat.1001261>.
- Liu S, Wang Q, Liu N, Luo H, He C, An B. The histone deacetylase HOS2 controls pathogenicity through regulation of melanin biosynthesis and appressorium formation in *Colletotrichum gloeosporioides*. *Phytopathol Res.* 2022;4:21. <https://doi.org/10.1186/s42483-022-00126-0>.
- Ma H, Li L, Gai Y, Zhang X, Chen Y, Zhuo X, et al. Histone acetyltransferases and deacetylases are required for virulence, conidiation, DNA damage repair, and multiple stresses resistance of *Alternaria alternata*. *Front Microbiol.* 2021;12: 783633. <https://doi.org/10.3389/fmicb.2021.783633>.
- Mehta N, Baghela A. Quorum sensing-mediated inter-specific conidial anastomosis tube fusion between *Colletotrichum gloeosporioides* and *C. siamense*. *IMA Fungus.* 2021;12:7. <https://doi.org/10.1186/s43008-021-00058-y>.
- O’Connell RJ, Thon MR, Hacquard S, Amyotte SG, Kleemann J, Torres MF, et al. Lifestyle transitions in plant pathogenic *Colletotrichum* fungi deciphered by genome and transcriptome analyses. *Nat Genet.* 2012;44(9):1060–5. <https://doi.org/10.1038/ng.2372>.
- Oliveira Silva A, Aliyeva-Schnorr L, Wirsal SGR, Deising HB. Fungal pathogenesis-related cell wall biogenesis, with emphasis on the maize anthracnose fungus *Colletotrichum graminicola*. *Plants.* 2022;11(7):849. <https://doi.org/10.3390/plants11070849>.
- Olsson TG, Ekwall K, Allshire RC, Sunnerhagen P, Partridge JF, Richardson WA. Genetic characterisation of hda1+, a putative fission yeast histone deacetylase gene. *Nucleic Acids Res.* 1998;26(13):3247–54. <https://doi.org/10.1093/nar/26.13.3247>.
- Pathan M, Keerthikumar S, Ang CS, Gangoda L, Quek CY, Williamson NA, et al. FunRich: an open access standalone functional enrichment and interaction network analysis tool. *Proteomics.* 2015;15(15):2597–601. <https://doi.org/10.1002/pmic.201400515>.

- Pidroni A, Faber B, Brosch G, Bauer I, Graessle S. A class 1 histone deacetylase as major regulator of secondary metabolite production in *Aspergillus nidulans*. *Front Microbiol*. 2018;9:2212. <https://doi.org/10.3389/fmicb.2018.02212>.
- Pijnappel WW, Schaft D, Roguev A, Shevchenko A, Tekotte H, Wilm M, et al. The *S. cerevisiae* SET3 complex includes two histone deacetylases, Hos2 and Hst1, and is a meiotic-specific repressor of the sporulation gene program. *Genes Dev*. 2001;15(22):2991–3004. <https://doi.org/10.1101/gad.207401>.
- Podila GK, Rogers LM, Kolattukudy PE. Chemical signals from avocado surface wax trigger germination and appressorium formation in *Colletotrichum gloeosporioides*. *Plant Physiol*. 1993;103(1):267–72. <https://doi.org/10.1104/pp.103.1.267>.
- Rockenbach MF, Velho AC, Gonçalves AE, Mondino PE, Alaniz SM, Stadnik MJ. Genetic structure of *Colletotrichum fructicola* associated to apple bitter rot and Glomerella leaf spot in southern Brazil and Uruguay. *Phytopathology*. 2016;106(7):774–81. <https://doi.org/10.1094/PHYTO-09-15-0222-R>.
- Shang S, Liang X, Liu G, Zhang S, Lu Z, Zhang R, et al. Histological and ultra-structural characterization of the leaf infection events of *Colletotrichum fructicola* on *Malus domestica* 'Gala'. *Plant Pathol*. 2020;69(3):538–48. <https://doi.org/10.1111/ppa.13141>.
- Studt L, Schmidt FJ, Jahn L, Sieber CM, Connolly LR, Niehaus EM, et al. Two histone deacetylases, Ffhda1 and Ffhda2, are important for *Fusarium fujikuroi* secondary metabolism and virulence. *Appl Environ Microbiol*. 2013;79(24):7719–34. <https://doi.org/10.1128/AEM.01557-13>.
- Taylor J. A necrotic leaf blotch and fruit rot of apple caused by a strain of *Glomerella cingulata*. *Phytopathology*. 1971;61:221–4. <https://doi.org/10.1094/Phyto-61-221>.
- Tessarz P, Kouzarides T. Histone core modifications regulating nucleosome structure and dynamics. *Nat Rev Mol Cell Biol*. 2014;15(11):703–8. <https://doi.org/10.1038/nrm3890>.
- Velho AC, Stadnik MJ, Wallhead M. Unraveling *Colletotrichum* species associated with Glomerella leaf spot of apple. *Trop Plant Pathol*. 2019;44(2):197–204. <https://doi.org/10.1007/s40858-018-0261-x>.
- Wang A, Kurdistani SK, Grunstein M. Requirement of Hos2 histone deacetylase for gene activity in yeast. *Science*. 2002;298(5597):1412–4. <https://doi.org/10.1126/science.1077790>.
- Wang CX, Zhang ZF, Li BH, Wang HY, Dong XL. First report of Glomerella leaf spot of apple caused by *Glomerella cingulata* in China. *Plant Dis*. 2012;96(6):912. <https://doi.org/10.1094/PDIS-11-11-0987-PDN>.
- Wang W, Liang X, Zhang R, Gleason ML, Sun G. Liquid shake culture overcomes solid plate culture in inducing conidial production of *Colletotrichum* isolates. *Australas Plant Path*. 2017;46(3):285–7. <https://doi.org/10.1007/s13313-017-0490-3>.
- Weir BS, Johnston PR, Damm U. The *Colletotrichum gloeosporioides* species complex. *Stud Mycol*. 2012;73(1):115–80. <https://doi.org/10.3114/sim0011>.
- Wirén M, Silverstein RA, Sinha I, Walfridsson J, Lee HM, Laurenson P, et al. Genomewide analysis of nucleosome density histone acetylation and HDAC function in fission yeast. *EMBO J*. 2005;24(16):2906–18. <https://doi.org/10.1038/sj.emboj.7600758>.

Ready to submit your research? Choose BMC and benefit from:

- fast, convenient online submission
- thorough peer review by experienced researchers in your field
- rapid publication on acceptance
- support for research data, including large and complex data types
- gold Open Access which fosters wider collaboration and increased citations
- maximum visibility for your research: over 100M website views per year

At BMC, research is always in progress.

Learn more biomedcentral.com/submissions

